Published in Optics Letters 42, issue 22, 4651-4654, 2017
which should be used for any reference to this work

Carrier-envelope offset stabilization of a GHz repetition rate femtosecond laser using opto-optical modulation of a SESAM

SARGIS HAKOBYAN,[1,*] VALENTIN J. WITTWER,[1] KUTAN GÜREL,[1] ALINE S. MAYER,[2] STÉPHANE SCHILT,[1] AND THOMAS SÜDMEYER[1]

[1]Laboratoire Temps-Fréquence, Université de Neuchâtel, CH-2000 Neuchâtel, Switzerland
[2]Department of Physics, Institute of Quantum Electronics, ETH Zurich, CH-8093 Zürich, Switzerland
*Corresponding author: sargis.hakobyan@unine.ch

We demonstrate, to the best of our knowledge, the first carrier-envelope offset (CEO) frequency stabilization of a GHz femtosecond laser based on opto-optical modulation (OOM) of a semiconductor saturable absorber mirror (SESAM). The 1.05-GHz laser is based on a Yb:CALGO gain crystal and emits sub-100-fs pulses with 2.1-W average power at a center wavelength of 1055 nm. The SESAM plays two key roles: it starts and stabilizes the mode-locking operation and is simultaneously used as an actuator to control the CEO frequency. This second functionality is implemented by pumping the SESAM with a continuous-wave 980-nm laser diode in order to slightly modify its nonlinear reflectivity. We use the standard f-to-$2f$ method for detection of the CEO frequency, which is stabilized by applying a feedback signal to the current of the SESAM pump diode. We compare the SESAM-OOM stabilization with the traditional method of gain modulation via control of the pump power of the Yb:CALGO gain crystal. While the bandwidth for gain modulation is intrinsically limited to ~250 kHz by the laser cavity dynamics, we show that the OOM provides a feedback bandwidth above 500 kHz. Hence, we were able to obtain a residual integrated phase noise of 430 mrad for the stabilized CEO beat, which represents an improvement of more than 30% compared to gain modulation stabilization.

OCIS codes: (140.4050) Mode-locked lasers; (140.3425) Laser stabilization; (120.3940) Metrology.

Optical frequency combs from mode-locked lasers [1–3] constitute a versatile tool for various applications such as optical frequency metrology [4,5], atomic clocks [6,7], or broadband high-resolution spectroscopy [8,9]. Some applications, e.g., the generation of ultra-low phase noise microwave signals by optical-to-microwave frequency division [10,11] or the calibration of astronomical spectrographs [12,13], benefit from the use of frequency combs with a high repetition rate in the multi-GHz range owing to their high power per comb mode and ease of access to individual optical lines. Most applications also require full-frequency comb stabilization, i.e., the two degrees of freedom, the repetition rate f_{rep}, and the carrier-envelope offset (CEO) frequency f_{CEO} need to be phase-coherently stabilized. The phase-stabilization of the CEO beat is usually the most challenging part. Since the CEO noise intrinsically scales with the repetition rate [14], the challenge is particularly pronounced for GHz repetition rate lasers. Traditionally, CEO stabilization is achieved using a phase-locked loop with feedback applied to the pump power of the femtosecond laser after detection of the CEO beat using nonlinear f-to-$2f$ interferometry [1]. This method is particularly suitable for diode-pumped femtosecond lasers, such as fiber lasers or diode-pumped solid-state lasers (DPSSLs), for which the injection current of the pump diode can be directly modulated. However, the stabilization bandwidth is fairly limited by the cavity dynamics. The latter is partially determined by the upper-state lifetime of the gain material, which is typically in the range of a few μs to a few ms for the most common crystals or glasses gain materials doped with erbium or ytterbium ions. Therefore, alternative stabilization methods have been proposed to overcome this limitation and enhance the stabilization bandwidth, thus improving the locking performance. Modulation of the stimulated emission in a co-doped Yb:Er:glass laser has been reported [15] where the gain material was additionally illuminated by modulated laser light at a wavelength within the gain bandwidth of the crystal, which enabled circumventing the low-pass filtering effect originating from the slow Yb^{3+} to Er^{3+} energy transfer mechanism. A different approach is based on the use of intracavity loss modulation, which was first demonstrated using a reflective graphene electro-optic modulator [16]. In 2013, we demonstrated, to the best of our knowledge, the first CEO control by opto-optical modulation (OOM) of a semiconductor saturable absorber mirror (SESAM). We used an Er:Yb:glass SESAM mode-locked DPSSL operating at a wavelength of 1.5 μm with a repetition rate of 75 MHz [17]. An additional continuous-wave beam from a diode laser was focused onto the SESAM slightly changing its reflectivity as a function of the incident power, thus acting as a fast loss modulator for the intra-cavity pulses due to the short SESAM response time. In comparison to the traditional gain modulation, the OOM showed strong improvements in terms of CEO modulation bandwidth and residual integrated phase noise of the locked CEO beat (65 mrad versus 720 mrad).

Here, we present, to the best of our knowledge, the first CEO stabilization of a DPSSL with a GHz repetition rate via OOM of a SESAM. In our previous OOM demonstration, realized with a low repetition rate laser, the bandwidth necessary for a tight CEO lock amounted to only a few kHz. For the CEO stabilization of our current GHz oscillator, the bandwidth requirement is more than an order of magnitude larger and thus represents a key test for the viability of the OOM method. We show a record high stabilization bandwidth of 500 kHz for a 1-μm Yb-based DPSSL. A tight locking of the CEO beat was achieved both for gain modulation and OOM, but a more than 30% reduction of the residual integrated phase noise of the locked CEO beat was achieved with the OOM.

The overall experimental setup is shown in Fig. 1. We used the same laser that we recently fully stabilized by cavity length control using a piezo-electrical transducer (for f_{rep}) and gain pump power modulation (for f_{CEO}) [18]. The Yb:CALGO laser is pumped by a commercial, spatially multimode, pump diode array (LIMO F100-DL980-EX1930), which is wavelength-stabilized by a volume holographic grating. This pumping scheme offers a straightforward way to scale up the output power of the laser, as we are currently using only 7.7 W out of the total diode output power of 30 W available in the s-polarization. However, multimode pumping tends to add extra noise compared to the low-noise operation of power-limited single-mode pump diodes, which increases the challenge to achieve CEO stabilization. The Yb:CALGO laser emits sub-100-fs optical pulses centered at 1055 nm with an optical bandwidth (full width at half-maximum, FWHM) of 17 nm, a repetition rate of 1.05 GHz, and a maximum average output power of 2.1 W. The laser has two output beams. One of them was used for f_{CEO} detection and stabilization (see Fig. 1), while the other one is available for further experiments. For CEO detection, an average power of 670 mW was directly launched into a photonic crystal fiber (PCF, model NL-3.2-945 from NKT Photonics) with a coupling efficiency of 80% without any pulse compression or amplification. As an alternative to a PCF, the use of a Si_3N_4 waveguide for octave-spanning supercontinuum generation for f_{CEO} detection was reported in a similar laser using much less pulse peak power [19]. The PCF used in our setup has a length of 1 m and a zero dispersion wavelength of 945 nm. The coherent octave-spanning supercontinuum (SC) spectrum at the output of the PCF was sent to an f-to-$2f$ interferometer for f_{CEO} detection. The CEO beat detected at 680 nm with a silicon avalanche photodiode showed a signal-to-noise ratio (SNR) of 40 dB (at 10-kHz resolution bandwidth) at a frequency of $f_{\mathrm{CEO}} \approx 266$ MHz. This signal was band-pass filtered and frequency down-converted to 21 MHz by mixing with the 245-MHz signal of a synthesizer. The resulting signal was compared in a digital phase detector to a 21-MHz reference signal from another synthesizer. The error signal was sent to a proportional-integral-derivative (PID) servo-controller (Vescent D2-125) and feedback was applied either to the laser pump diode (gain modulation, Diode #1 and channel #1 in Fig. 1) or to the SESAM pump power (SESAM-OOM, Diode #2 and channel #2 in Fig. 1).

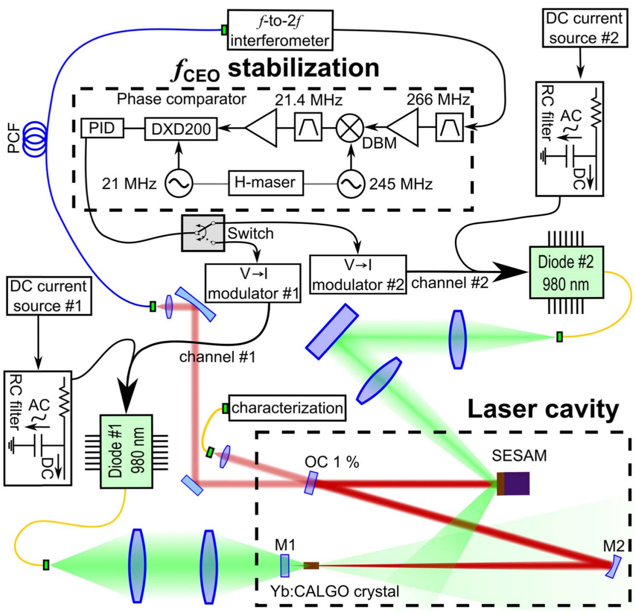

Fig. 1. Experimental setup. A pair of DC current sources, 980-nm pump diodes, RC filters, and V–I modulators are used to pump the GHz laser crystal and SESAM, respectively, and to stabilize the f_{CEO} via gain modulation (channel #1) or SESAM-OOM (channel #2). The laser cavity shown in the lower-right corner has two output beams. The generation of the error signal for f_{CEO} stabilization is shown in the upper part of the scheme. DBM, double-balanced mixer; PCF, photonic crystal fiber; PID, proportional-integral-derivative servo-controller; green/red/light-red lines, free-space optical beams (pump/intra-cavity/outputs); yellow/blue lines, optical fibers (single-mode/PCF); and black lines, electrical connections.

The OOM was implemented by pumping the SESAM with an s-polarized 980.9-nm laser beam (Diode #2 in Fig. 1) focused onto the SESAM at an incidence angle of ∼45°. Here, we used for convenience the same type of pump diode as for the laser crystal, but a standard low-cost, low-power, laser diode could be used as well (CEO stabilization is achieved for less than 200 mW output power). The present pump diode has a spectral width of ∼0.2 nm. The OOM pump beam was aligned to overlap with the intra-cavity laser pulses onto the SESAM with a spot diameter of ∼300 μm. From simulations of the electrical field propagation of the OOM pump light inside the SESAM structure, an absorption of only 1.3% was calculated in the InGaAs quantum well absorber. Another 1.3% is transmitted through the entire structure and eventually gets scattered at the unpolished back surface of the GaAs substrate. Finally, the remaining 97.4% is simply reflected on the Bragg mirror and does not play any role for the OOM. It is important to note that no material, other than the quantum well, notably absorbs the OOM pump laser light since the GaAs SESAM material is transparent at the 980-nm pump wavelength, which minimizes undesired temperature-induced effects. The SESAM has a saturation fluence of 10.69 μJ/cm^2 and is operated at an intra-cavity laser fluence of 93.6 μJ/cm^2, close to the maximum of its nonlinear reflectivity curve. Hence, the maximum reflectivity change produced by the pump light can be at most 0.1%. From the induced frequency change of f_{CEO}, the reflectivity change produced by the pump light is estimated to be two orders of magnitude smaller than the 1.15% SESAM modulation depth.

To enable fast modulation of the pump diodes (for gain or SESAM pumping), we used high-bandwidth voltage-to-current (V–I) converters developed in our institute (V–I modulator #1 and #2 in Fig. 1). Those V–I modulators were connected in parallel to the high DC current sources of the pump diodes. An RC filter was used to prevent any cross talk between each DC current source and modulator and to reduce the current noise induced by the DC sources (see more details in Ref. [18]).

To characterize the OOM operation, we first checked the modulation bandwidth of the OOM pump laser diode achieved with the V–I modulator by measuring the transfer functions of its output power for a sine modulation of its drive current (black curves in Fig. 2). Then, we measured the transfer function of f_{CEO} for a sine modulation with a peak-to-peak amplitude of 190 mW of the OOM pump power using a frequency discriminator [20] and a lock-in amplifier. This measurement was performed at two different OOM average pump power levels of 212 mW and 763 mW (dark and light red curves, respectively, in Fig. 2). For comparison, the figure also displays the measured transfer function of f_{CEO} for a modulation of the Yb:CALGO laser pump power (blue curves in Fig. 2).

The OOM pump laser diode has a modulation bandwidth of ~800 kHz (defined by the 90° phase shift in the transfer function of the diode output power). The CEO bandwidth for gain modulation is limited to ~280 kHz by the dynamics of the mode-locked laser cavity [18]. The OOM overcomes this limitation and achieves a CEO modulation bandwidth more than two times larger, with a 90° phase shift reached at ~630 kHz. At high average pump power incident onto the SESAM, a phase reversal of 180° is observed at low frequency in the transfer function of f_{CEO} in comparison to the low-power case (compare the red and light red curves in Fig. 2(b) below 10 kHz), while above ~10 kHz the phase of the transfer function is equal in both cases. This behavior is believed to result from a dominant slow thermal effect resulting from spurious pump light absorption outside of the quantum well occurring at high average OOM pump power. In contrast, the desired optically induced change in the SESAM reflectivity prevails at lower average power. The SESAM was neither cooled nor actively temperature stabilized. To further investigate this phase reversal, we measured the phase of the change in f_{CEO} induced by a slow SESAM pump modulation of 10 Hz with a constant peak-to-peak amplitude of 190 mW at different average pump power levels ranging from ~0.1 W to 1.2 W. In Fig. 3, a clear phase reversal is observed at an average power of ~400 mW incident onto the SESAM.

The response of f_{CEO} with respect to the OOM pump power is in the range of 1 kHz/mW. This value is 200 times lower compared to the typical tuning coefficient of f_{CEO} with the laser pump power (gain modulation) in our laser [18]. Nevertheless, the achievable CEO tuning was sufficient for f_{CEO} locking by means of the OOM only. The stabilization was successful for low average power incident onto the SESAM (typ. 210 mW). However, CEO stabilization was not possible at high average pump power incident onto the SESAM as a result of the inadequate CEO transfer function resulting from the low-frequency phase reversal as previously observed in a 1.5-μm DPSSL affected by similar CEO dynamics [21].

The frequency noise power spectral density (FN-PSD) measured for the free-running (light green), gain-stabilized (blue), and OOM-stabilized (red) CEO beat is shown in Fig. 4. While the free-running CEO beat has a FWHM of ~500 kHz, the OOM stabilization leads to a tight lock characterized by a coherent peak with an SNR of ~60 dB at 1-Hz resolution bandwidth in the CEO beat measured in-loop [see Fig. 5(b)]. The residual integrated phase noise amounts to 430 mrad [10 Hz–1 MHz] (Fig. 4, right axis), which is an improvement

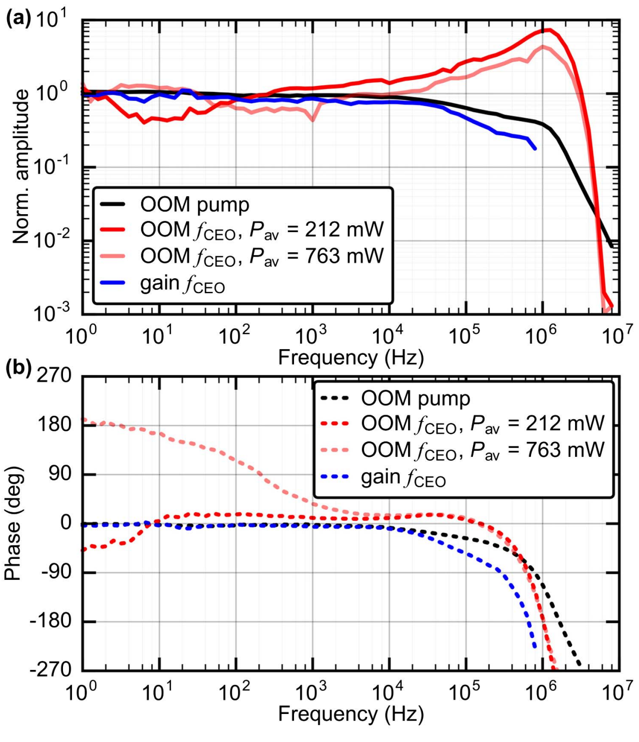

Fig. 2. Relative amplitude (a) and phase (b) of the transfer functions (TFs) of f_{CEO} for a modulation of the OOM pump at two different average powers P_{av} incident onto the SESAM: 212 mW (red) and 763 mW (light red). The TFs of the f_{CEO} for gain modulation (blue), and of the OOM pump laser power (black) are also shown for comparison.

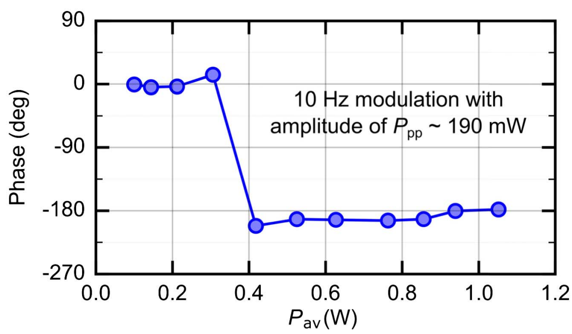

Fig. 3. Phase of the response of f_{CEO} to a 10-Hz modulation of the SESAM-OOM pump power as a function of the average optical power P_{av} incident onto the SESAM, showing a phase reversal point at $P_{av} \approx 400$ mW. A constant modulation amplitude of 190 mW (peak-to-peak value) was used in all cases.

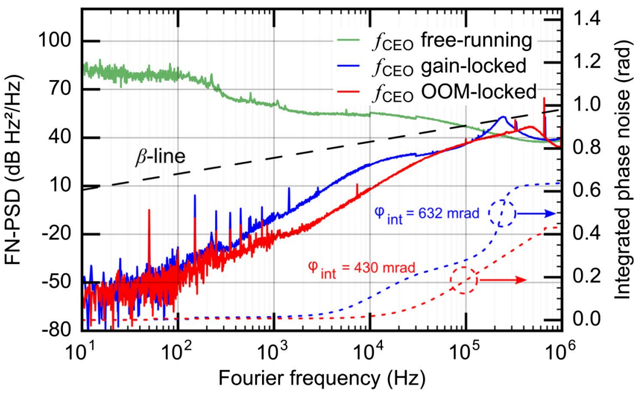

Fig. 4. Frequency noise power spectral density (FN-PSD) of the CEO beat obtained in free-running conditions (green), for the CEO beat stabilized by gain modulation (blue), and by SESAM-OOM (red). The corresponding integrated phase noise is shown as a function of the upper cut-off frequency (right vertical axis).

by more than 30% compared to stabilizing the CEO of this laser via gain modulation, where we achieved 632 mrad. A stabilization bandwidth of 500 kHz assessed from the servo bump in the CEO FN-PSD was obtained with the OOM. This is two times higher than the ~250-kHz bandwidth of the gain-modulation stabilization. Even higher stabilization bandwidths were possible with the OOM, typically up to ~580 kHz; however, the best noise properties were obtained with the 500-kHz stabilization bandwidth shown in Fig. 4.

The RF spectra of the free-running and stabilized CEO beats are shown in Fig. 5. The side peaks present in the spectrum at around ±310 kHz and ±620 kHz are believed to be of electrical origin (they are also present in the CEO spectrum obtained by gain modulation) and have a negligible contribution to the integrated phase noise of the stabilized CEO beat.

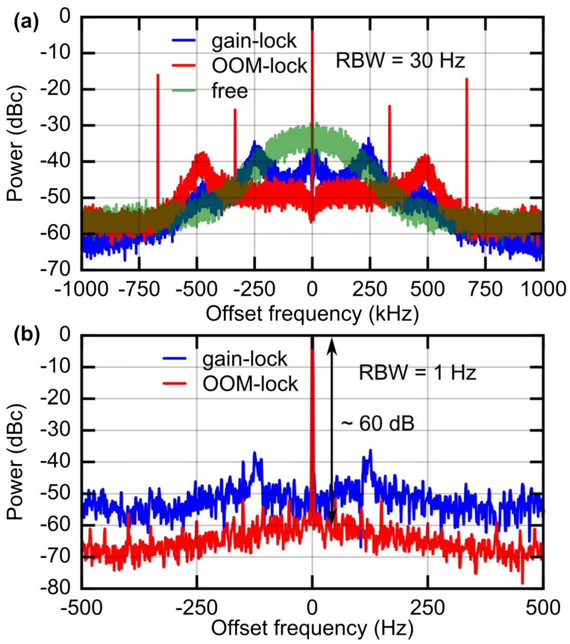

Fig. 5. (a) RF spectrum of the CEO beat in free-running mode (green), stabilized with gain modulation (blue), and with SESAM-OOM (red), showing a twofold enhancement of the stabilization bandwidth. (b) Zoom on the coherent peak over a total span of 1 kHz showing an SNR of 60 dB (1-Hz resolution bandwidth) for OOM stabilization.

In conclusion, we have presented, to the best of our knowledge, the first SESAM-OOM self-referenced stabilization of a GHz DPSSL, overcoming the cavity dynamics limitation and extending the stabilization bandwidth by a factor of more than two. As a result, the CEO residual integrated phase noise was reduced by more than 30% compared to the traditional gain modulation stabilization. These results demonstrate that SESAMs are reliable components not only for mode-locking, but they also can serve as fast loss modulators for frequency comb stabilization, which can overcome the limitations of the standard gain modulation.

Funding. Kommission für Technologie und Innovation (KTI) (17137.1, PFMN-NM).

REFERENCES

1. H. R. Telle, G. Steinmeyer, A. E. Dunlop, J. Stenger, D. H. Sutter, and U. Keller, Appl. Phys. B **69**, 327 (1999).
2. D. J. Jones, S. A. Diddams, J. K. Ranka, A. Stentz, R. S. Windeler, J. L. Hall, and S. T. Cundiff, Science **288**, 635 (2000).
3. A. Apolonski, A. Poppe, G. Tempea, C. Spielmann, T. Udem, R. Holzwarth, T. W. Hänsch, and F. Krausz, Phys. Rev. Lett. **85**, 740 (2000).
4. T. W. Hänsch, Rev. Mod. Phys. **78**, 1297 (2006).
5. J. Ye, H. Schnatz, and L. W. Hollberg, IEEE J. Sel. Top. Quantum Electron. **9**, 1041 (2003).
6. S. A. Diddams, T. Udem, J. C. Bergquist, E. A. Curtis, R. E. Drullinger, L. Hollberg, W. M. Itano, W. D. Lee, C. W. Oates, K. R. Vogel, and D. J. Wineland, Science **293**, 825 (2001).
7. U. Sterr, C. Degenhardt, H. Stoehr, C. Lisdat, H. Schnatz, J. Helmcke, F. Riehle, G. Wilpers, C. Oates, and L. Hollberg, C. R. Phys. **5**, 845 (2004).
8. S. Schiller, Opt. Lett. **27**, 766 (2002).
9. S. A. Diddams, L. Hollberg, and V. Mbele, Nature **445**, 627 (2007).
10. T. M. Fortier, M. S. Kirchner, F. Quinlan, J. Taylor, J. C. Bergquist, T. Rosenband, N. Lemke, A. Ludlow, Y. Jiang, C. W. Oates, and S. A. Diddams, Nat. Photonics **5**, 425 (2011).
11. X. Xie, R. Bouchand, D. Nicolodi, M. Giunta, W. Hänsel, M. Lezius, A. Joshi, S. Datta, C. Alexandre, M. Lours, P.-A. Tremblin, G. Santarelli, R. Holzwarth, and Y. L. Coq, Nat. Photonics **11**, 44 (2017).
12. C.-H. Li, A. J. Benedick, P. Fendel, A. G. Glenday, F. X. Kärtner, D. F. Phillips, D. Sasselov, A. Szentgyorgyi, and R. L. Walsworth, Nature **452**, 610 (2008).
13. T. Steinmetz, T. Wilken, C. Araujo-Hauck, R. Holzwarth, T. W. Hänsch, L. Pasquini, A. Manescau, S. D'Odorico, M. T. Murphy, T. Kentischer, W. Schmidt, and T. Udem, Science **321**, 1335 (2008).
14. B. R. Washburn, W. C. Swann, and N. R. Newbury, Opt. Express **13**, 10622 (2005).
15. L. Karlen, G. Buchs, E. Portuondo-Campa, and S. Lecomte, Opt. Lett. **41**, 376 (2016).
16. C.-C. Lee, C. Mohr, J. Bethge, S. Suzuki, M. E. Fermann, I. Hartl, and T. R. Schibli, Opt. Lett. **37**, 3084 (2012).
17. M. Hoffmann, S. Schilt, and T. Südmeyer, Opt. Express **21**, 30054 (2013).
18. S. Hakobyan, V. J. Wittwer, P. Brochard, K. Gürel, S. Schilt, A. S. Mayer, U. Keller, and T. Südmeyer, Opt. Express **25**, 20437 (2017).
19. A. Klenner, A. S. Mayer, A. R. Johnson, K. Luke, M. R. E. Lamont, Y. Okawachi, M. Lipson, A. L. Gaeta, and U. Keller, Opt. Express **24**, 11043 (2016).
20. S. Schilt, N. Bucalovic, L. Tombez, V. Dolgovskiy, C. Schori, G. Di Domenico, M. Zaffalon, and P. Thomann, Rev. Sci. Instrum. **82**, 123116 (2011).
21. N. Bucalovic, V. Dolgovskiy, M. C. Stumpf, C. Schori, G. Di Domenico, U. Keller, S. Schilt, and T. Südmeyer, Opt. Lett. **37**, 4428 (2012).